Clays and Clay Minerals, Vol. 46, No. 6, 658–669, 1998.

BURIAL DIAGENETIC PROCESSES AND CLAY MINERAL FORMATION IN THE MOLASSE ZONE OF UPPER AUSTRIA

SUSANNE GIER

Institute of Petrology, University of Vienna, Geozentrum, Althanstraße 14, 1090 Vienna, Austria

Abstract—Cores of pelitic sediments (Eocene-Miocene) of the drillings Puchkirchen 1 and Geretsberg 1 (Molasse Basin, Upper Austria) have been studied to determine the mineralogical and chemical changes taking place during burial diagenesis. Mineralogical and chemical investigations of the bulk samples show that the deepest samples of the profiles are derived from a different source area. In particular, there is an increase in kaolinite and chlorite with depth and a decrease in quartz related to the initial sedimentology and provenance.

Investigations of the <2 μm and <0.2 μm fractions of the profiles Puchkirchen 1 and Geretsberg 1 reveal the diagenetic overprint of the mineral constituents: The gradual illitization of mixed-layer illite–smectite, also reflected in an increase of K_2O and Al_2O_3, is displayed most prominently in the <0.2 μm fraction. The source for the Al and K is the dissolution of K-feldspar (<2 μm fraction), as indicated in many previous studies.

The I–S mixed-layer phases are randomly interlayered to a depth of 1600 m; from there on a regular interstratified I–S phase appears in coexistence with the randomly interlayered I–S mixed layer. The randomly oriented phase is still present in major amounts to depths of 2500 m, presumably as a result of the low geothermal gradient (2.9 °C/100 m) in the Molasse Basin.

The calculation of the structural formula of the end members illite and smectite from this series of I–S mixed-layer phases gave the following results:

Smectite:

$$K_{0.14}X^{+}_{0.44}(Al_{1.10}Mg_{0.46}Fe_{0.36}Ti_{0.01})Si_{4.03}O_{10}(OH)_2$$

Illite:

$$K_{0.44}X^{+}_{0.19}(Al_{1.26}Mg_{0.42}Fe_{0.38}Ti_{0.01})(Si_{3.52}Al_{0.48})O_{10}(OH)_2$$

The end-member interlayer charge for the smectite component (+0.58) is higher than reported for typical smectites (+0.32 to +0.47). It is suggested that the I–S phases of the Molasse Basin are probably intergrowths of 3 layer-silicate members: illite, low-charged smectite and high-charged smectite. The determined smectite end-member composition represents, therefore, an average for a variable 2-component smectite system. The charge-differences of the 2 smectites would likely reflect the differences in source material, which in turn would have led to the formation of different early, highly smectitic I–S phases in the sedimentary basin.

Key Words—Austria, Diagenesis, High-Charged Smectite, Illite–Smectite, Molasse Basin.

INTRODUCTION

Burial diagenetic processes of pelitic sediments have been the subject of numerous mineralogical investigations in Tertiary basins worldwide (Johns and Kurzweil 1979; Awwiller 1993; Sucha et al. 1993; Lynch 1997). Related to oil exploration, the initial investigations were intensive in the Gulf Coast region and the diagenetic reaction observed was: Smectite + Al^{3+} + K^{+} = illite + Si^{4+} (Hower et al. 1976). The transformation from smectite to illite was also related to petroleum migration processes due to the release of interlayer water (Powers 1967; Burst 1969; Perry and Hower 1972; Bruce 1984).

The published data from the Gulf of Mexico sedimentary basin were reinterpreted by Eberl (1993). Three reaction zones for illite formation with increasing depth were identified: K-ion exchange resulting in smectite transformation to illite in a shallow zone (1.85 to 3 km), illite neoformation from dissolution of coarser K-bearing phases and smectite by organic acids in a middle zone (3 to 4 km) and illite recrystallization from dissolution of less stable illite crystals and growth of more stable illite crystals during mineral ripening in the deepest zone (>4 km).

In Austria, clay mineral diagenesis was studied in the Vienna Basin by Kurzweil and Johns (1981) and Horton et al. (1985). The present study involves diagenetic development of the clay minerals in the Molasse Basin of Upper Austria, where different sediment sources are involved. The Molasse Zone (Figure 1) is situated north of the Alps; it belongs to the Alpine-Carpathian orogenic belt. The part of the Molasse Basin in Austria is 300 km long and its width varies between 5 and 50 km. During orogenesis, the basin accepted first the detrital sediments from the northern Bohemian Massif and then, as the alpine orogen rose, the sediments were derived from the south. The Molasse sediments were partly overthrusted by the nappe

https://doi.org/10.1346/CCMN.1998.0460606 Published online by Cambridge University Press

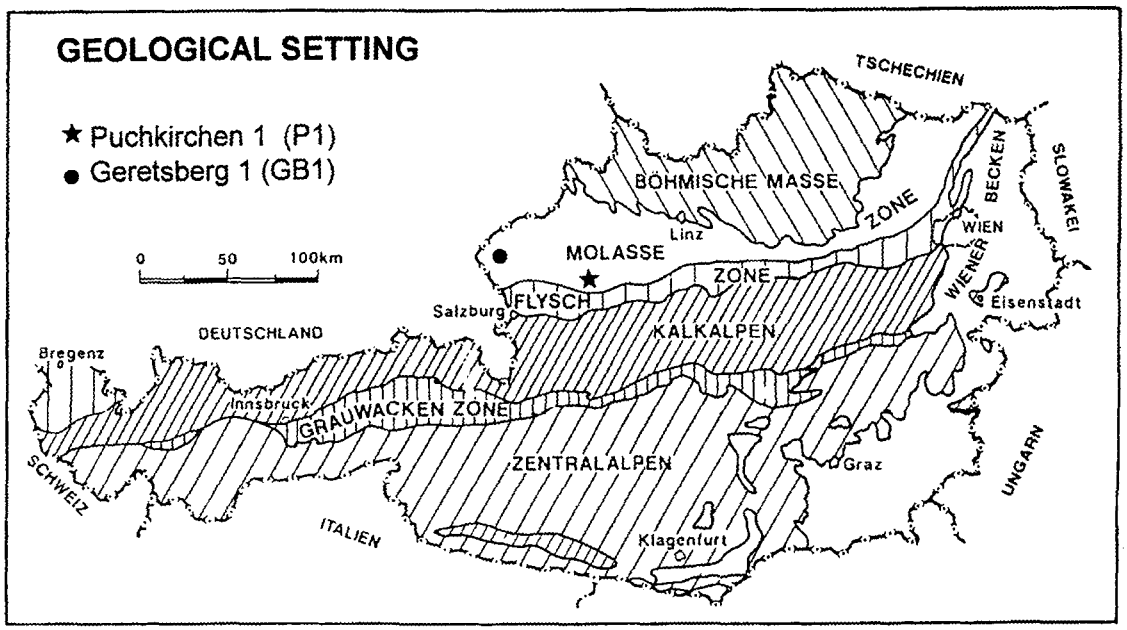

Figure 1. Geologic map and the locations of the drillings Puchkirchen 1 (P1) and Geretsberg 1 (GB1).

system of the Kalkalpen (Northern Calcareous Alps). The thickness of the Molasse sediments increases from north to south to 3000 m (Tollmann 1985). The age of the sediments ranges from Tertiary, where sedimentation started in Upper Eocene, to Quaternary (Malzer et al. 1993).

Two cores (Puchkirchen 1 and Geretsberg 1, Figure 1) of the Molasse Basin were analyzed to determine mineralogical and chemical changes with depth. The well cores were made available by the Rohöl-Aufsuchungs AG (RAG), an oil-exploration company of this region. The samples studied belong to the Haller, Puchkirchener and Rupelien series, to the Fishshale and to the Top limnic series of the Molasse Basin (Table 1). The depth interval investigated covers 590 to 2625 m. The geothermal gradient of the drillings Puchkirchen 1 and Geretsberg 1 is 2.9 °C/100 m (Figure 2). This gradient was calculated from data provid-

Table 1. Stratigraphy and depths of the core samples P (Puchkirchen 1, 2) and GB (Geretsberg 1).

Sample	Depth (m)	Stratigraphy	Series
1P1	590	Haller S.	L-Miocene
2P1	801	Haller S.	L-Miocene
3P1	1004	Haller S.	L-Miocene
4P1	1130	U. Puchkirchener S.	U-Oligocene-L-Miocene
5P1	1274	U. Puchkirchener S.	U-Oligocene-L-Miocene
6P1	1560	U. Puchkirchener S.	U-Oligocene-L-Miocene
7P1	1622	U. Puchkirchener S.	U-Oligocene-L-Miocene
8P1	1885	U. Puchkirchener S.	U-Oligocene-L-Miocene
9P1	2065	L. Puchkirchener S.	U-Oligocene
10P1	2297	L. Puchkirchener S.	U-Oligocene
11P1	2378	L. Puchkirchener S.	U-Oligocene
12P1	2475	Rupel	M-Oligocene
13P2	2583	Fishshale	Latdorfian
14P2	2625	Top Limnic S.	U-Eocene
27GB1	912	Haller S.	L-Miocene
28GB1	1093	Haller S.	L-Miocene
29GB1	1323	Haller S.	L-Miocene
30GB1	1530	U. Puchkirchener S.	U-Oligocene-L-Miocene
31GB1	1709	U. Puchkirchener S.	U-Oligocene-L-Miocene
32GB1	1918	L. Puchkirchener S.	U-Oligocene
33GB1	2110	L. Puchkirchener S.	U-Oligocene
34GB1	2247	Tonmergel Rupel	M-Oligocene
35GB1	2420	Fishshale	Latdorfian

https://doi.org/10.1346/CCMN.1998.0460606 Published online by Cambridge University Press

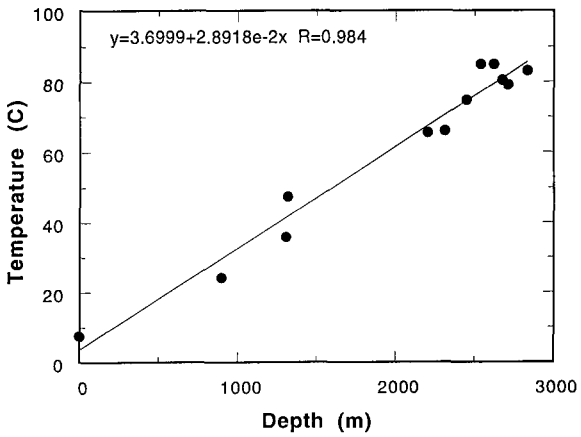

Figure 2. Calculated geothermal gradient based on data from P1 and GB1.

ed by RAG AG. The temperature in the wells was measured after temperature equilibration.

The main investigations concentrate on the <2 μm and <0.2 μm fractions, where mixed-layer formation is best revealed. The <0.2 μm fraction was characterized mineralogically and chemically in detail for the purpose of calculating the structural formulas of the mixed-layer minerals and their end members smectite and illite.

SAMPLE PREPARATION

The outer 0.5 cm of each core was removed to avoid possible contamination from drilling fluid. The samples were crushed to a size of 3 mm and the carbonates and free iron oxides were dissolved and removed with 0.1 *M* EDTA solution (pH 4.5) at 50 °C (Glover 1961; Kohler and Wewer 1980). They were also treated 6 min with a 400 W ultrasonic probe (approximately 30 g sample in 300 mL fluid) for further disaggregation. The samples were saturated with 1 *M* NaCl solution to exchange the naturally adsorbed cations by Na to avoid flocculation, and afterwards washed repeatedly to remove excess chloride. The <2 μm fractions were separated by sedimentation, the <0.2 μm fractions by timed centrifugation. The resulting suspensions were concentrated by evaporation and the still wet samples were freeze-dried.

Oriented preparations of the <0.2 μm fractions for XRD were made by dispersing approximately 3 mg of clay separate in 1 mL of water, pipetting the suspension onto a round glass slide (diameter 2.5 cm) and drying at room temperature. Oriented XRD mounts were analyzed air-dried and after vapor solvation with ethylene glycol at 60 °C for 12 h.

MINERALOGY

Bulk Samples

The mineralogical compositions of the bulk samples were determined by X-ray powder diffraction (XRD). Diffraction data were collected with a Philips diffractometer (PW 1710, goniometer PW 1820), Cu*K*α radiation (45 kV, 35 mA), step scan (step size 0.02, 1 s per step). Semiquantitative estimates of the mineral constituents were made following the method of Schultz (1964), which implies error limits of ±10% for phases present in an amount greater than 15% of the sample. The composition of the shallower samples (Miocene to Middle Oligocene) is very uniform, containing quartz, plagioclase, K-feldspar, calcite, dolomite, gypsum, pyrite and the clay minerals smectite, kaolinite, mica and chlorite. The mineralogical composition of the 2 deepest samples of the profile Puchkirchen (Lower Oligocene and Upper Eocene) and the deepest sample of the profile Geretsberg (Lower Oligocene) is different: these samples have a very high content of kaolinite. This difference in the mineralogical compositions of the shales is due to paleogeographically different source areas. At the time of the Upper Eocene and part of the Lower Oligocene, the sediments were derived from the north, the Bohemian Massif, but with the uplift of the Alps, the direction and provenance of sedimentation changed, coming from the alpine area in the south (Kurzweil 1973). The source of kaolinite was the weathering of feldspar-rich rocks as they occur in the Bohemian Massif. Because of the different mineralogical composition of the older sediments, only the samples derived from the alpine source area were used for the investigations concerning the diagenetic changes in clay minerals with depth.

<2 μm Fraction

The mineralogy of this size fraction is similar to the composition of the bulk samples, except for the contents of calcite and dolomite, which were dissolved during the preparation with EDTA. In the XRD diagrams the mixed-layer mineral I–S is revealed for the first time.

Figure 3 shows the depth distribution of non-clay minerals in the 2 drillings. Quartz and K-feldspar decrease somewhat with depth in both profiles, while total clay mineral content remains essentially constant in the <2 μm fractions.

Figure 4, showing clay mineral distribution with depth, indicates an increase in discrete illite and chlorite with concomitant decrease in I–S mixed layer phase in the <2 μm fractions in both the Puchkirchen and Geretsberg profiles. The increase in kaolinite in the older sediments was noted previously.

<0.2 μm Fraction

Figure 5 shows XRD patterns of <0.2 μm fraction samples from different depths (801 m, 1622 m, 2378 m). The <0.2 μm fractions are essentially I–S mixed-layer phases with minor amounts of discrete mica, kaolinite and chlorite present. The strong, broad reflection at 17 Å indicates random interstratification of the

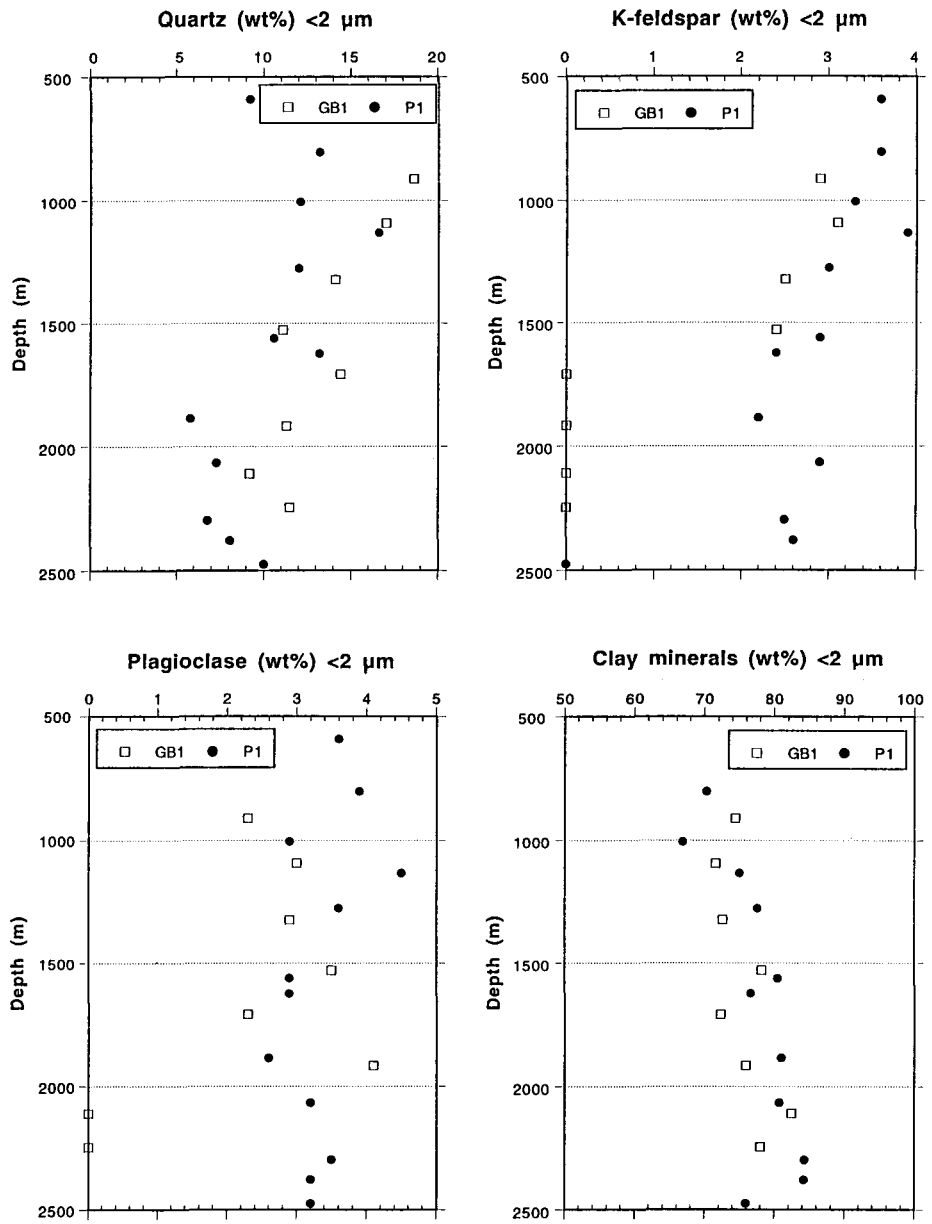

Figure 3. Distribution of the non-clay minerals of the <2 µm fraction with depth in P1 and GB1.

I–S mixed layer (Moore and Reynolds 1989). Additionally, the deeper samples show a weak reflection at around 27 Å, which could be the 001 of the superstructure reflection, but there is no other evidence for R1 ordering. The percentage of illite in the mixed layer mineral I–S was determined by the °2θ difference values of the peak positions 001/002 and 002/003 (Moore and Reynolds 1989). The precise peak positions were found with support of the "fit profile" option of the Philips APD-software 3.5B (1992).

As shown in Figure 6, the relative proportions of illite layers in the I–S phases increase with depth to a maximum of 70% illite layers. The I–S mixed layers are randomly oriented to a depth of 1600 m and an illite content in I–S of about 52%. In the depth range 1600 to 2500 m of the profiles, there is evidence of ordered I–S in coexistence with the randomly interstratified I–S. The randomly oriented phase is still present in major amounts in a depth of 2500 m, presumably a result of the low geothermal gradient (2.9 °C/100 m) in the Molasse Basin.

Both the mixed-layer I–S and impurities had to be quantified for the chemical formula calculations. The XRD peaks selected for the quantification of the <0.2

https://doi.org/10.1346/CCMN.1998.0460606 Published online by Cambridge University Press

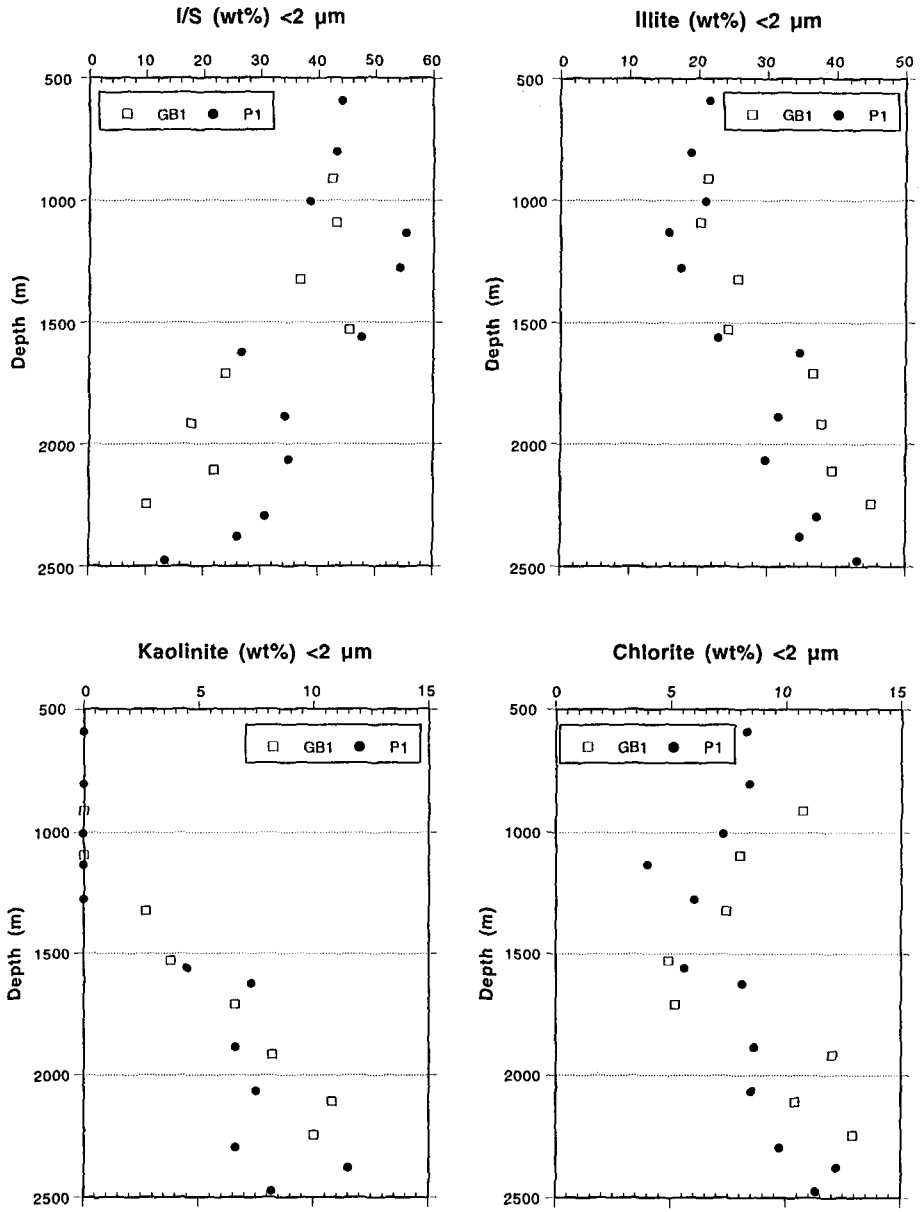

Figure 4. Clay mineral-distribution of the <2 µm fraction with depth in P1 and GB1.

µm fraction were the I_{002}–S_{003} peak, the illite 002 peak (17.7 °2θ), the chlorite 003 peak (18.8 °2θ) and the kaolinite 003 peak (37.7 °2θ). The peak value for the mineral was corrected by dividing its area by its mineral intensity factor (MIF) (Reynolds 1989; Moore and Reynolds 1989). To verify the calculated quantities, the experimental diagrams were compared with theoretical ones produced by NEWMOD© (Reynolds 1985), a computer program for the simulation of mixed-layer patterns and admixing of layer silicate impurities.

Examination of the *d*(060) values for this clay fraction indicates dioctahedral phases only: the *d*-values range from 1.4968 Å to 1.5026 Å. There appears to be a slight trend with depth to higher values, as expected with increasing tetrahedral substitutions.

CHEMISTRY

Major-element chemistry of whole-rock samples was measured by *X-ray fluorescence (XRF) analysis* (Philips PW 2400) for all major oxides. The results

https://doi.org/10.1346/CCMN.1998.0460606 Published online by Cambridge University Press

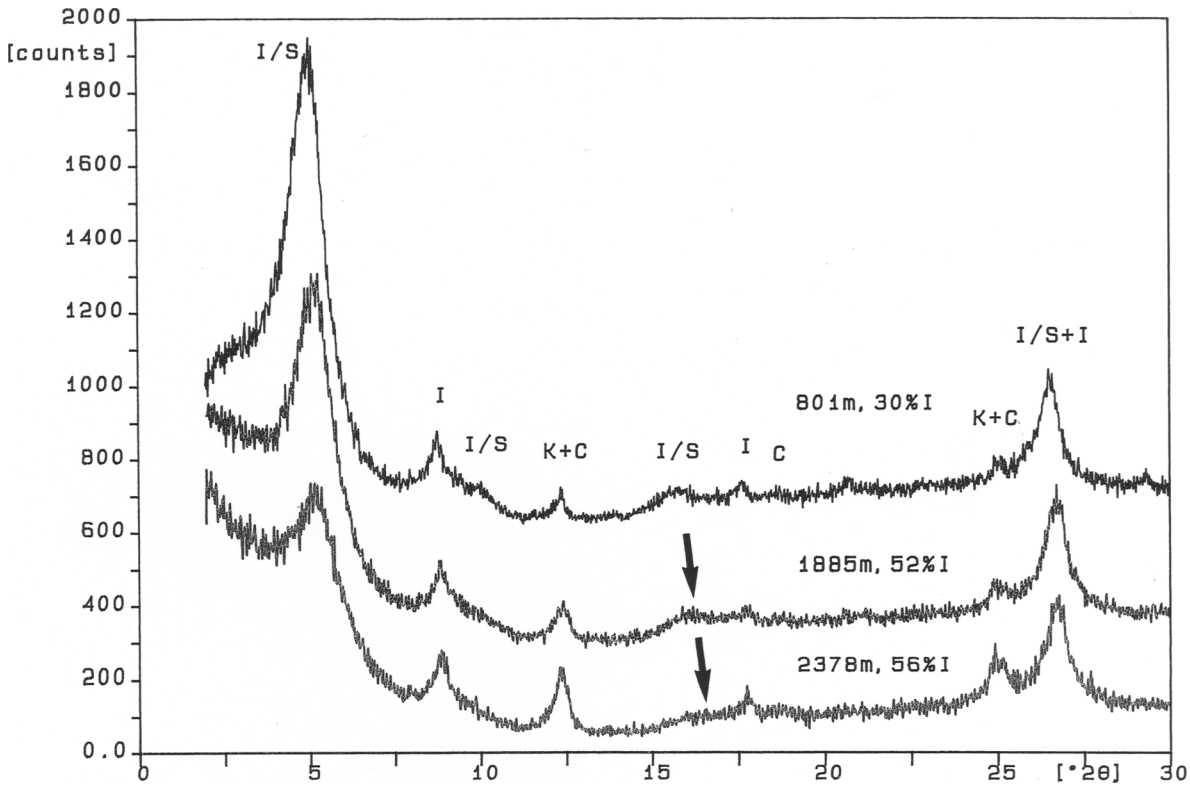

Figure 5. XRD patterns of oriented, EG-saturated <0.2 μm fraction samples. I/S = illite–smectite, I = illite, K = kaolinite, C = chlorite. Arrows show locations of I–S peaks.

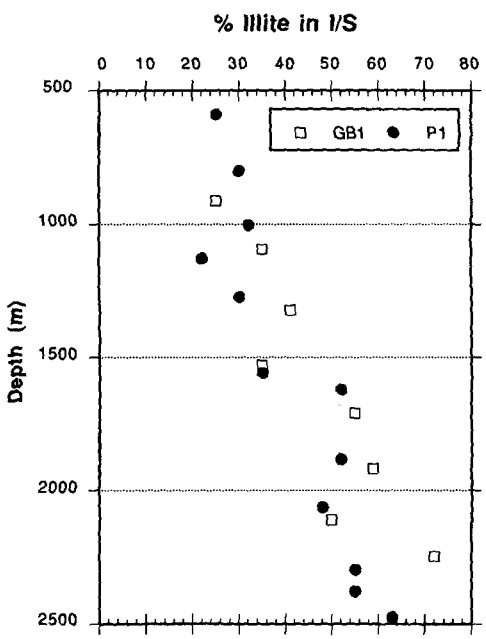

Figure 6. Percentage of illite layers in I–S with depth of P1 and GB1.

from bulk analysis reflect mineralogical changes within each profile.

In order to focus attention on compositional changes during diagenetic smectite-to-illite transformation, chemical analyses of the <0.2 μm fractions are emphasized. Because these samples, consisting of very pure I–S, were very small, it was necessary to use dissolution with NaOH (Köster 1979) coupled with inductively coupled plasma-atomic emission spectroscopy (ICP-AES) (Jobin Yvon JY70 Plus) analysis for these <0.2 μm samples. The quality of the analyses was assured by preparing and analyzing 2 standards, TB (Clay shale, Association Nationale 1989) and Brick clay (NBS standard reference material 679), exactly the same way as the samples. The relative error of the ICP analysis data for the elements was about ±5%.

The results of these analyses are plotted as a function of depth in Figure 7 for the Puchkirchen and Geretsberg profiles. There is an increase in Al_2O_3 and K_2O in both profiles and also a slight increase in MgO and Fe_2O_3, whereas SiO_2 stays about constant.

CATION EXCHANGE CAPACITY (CEC)

The CEC of the <0.2 μm fractions should give a measure of the interlayer charge of the smectite com-

https://doi.org/10.1346/CCMN.1998.0460606 Published online by Cambridge University Press

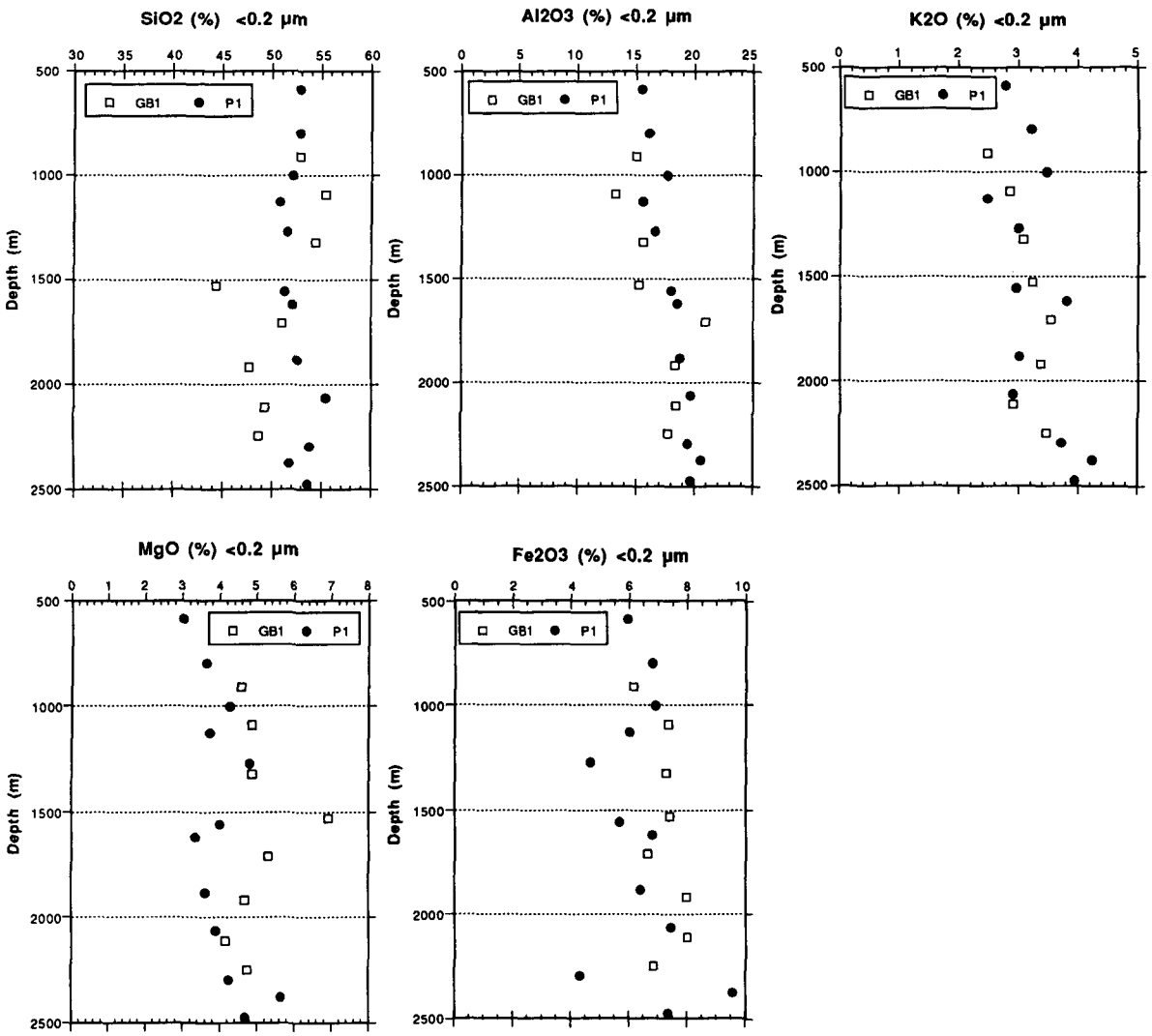

Figure 7. Distribution of the chemical components of the <0.2 µm fraction with depth for Puchkirchen 1 and Geretsberg 1.

ponents of the I–S phases. The CEC of the <0.2 µm clay fraction was determined after Busenberg and Clemency (1973). This method involves saturating the clay with ammonium ions, liberating the ammonium ions from the clay with sodium hydroxide and measuring the liberated NH_3 with a specific electrode. The CEC values (meq/100 g) measured are plotted as a function of percent smectite layers in Figure 8. The linearity of the plot shows that the ammonium exchange capacity is a function of the amount of smectite. When extrapolated to 100% smectite and 100% illite, the CEC value for smectite is 94.2 meq/100 g and 32.8 meq/100 g for illite.

This was the first evidence to suggest that the smectitic component of these I–S clays has an anomalously high interlayer charge, especially when compared to analogous sediments from the Vienna Basin (Horton et al. 1985). Because of the significance of this inference, the measurements were repeated and confirmed.

CALCULATION OF THE STRUCTURAL FORMULAS OF I–S AND THE END MEMBERS ILLITE AND SMECTITE

The chemical analyses of the I–S component of the <0.2 µm fractions provide the basis for calculation of structural formulas. For the calculations of the structural formulas of the pure mixed-layer minerals I–S, the determined amounts of the impurites kaolinite and chlorite (Table 2) had to be subtracted first from the chemical analyses of the <0.2 µm samples. Kaolinite was assumed to have the ideal composition (Jasmund and Lagaly 1993): SiO_2 46.55%, Al_2O_3 39.50%, H_2O 13.95%. For the correction of chlorite, a mineral of the following composition was used (Deer et al. 1962):

https://doi.org/10.1346/CCMN.1998.0460606 Published online by Cambridge University Press

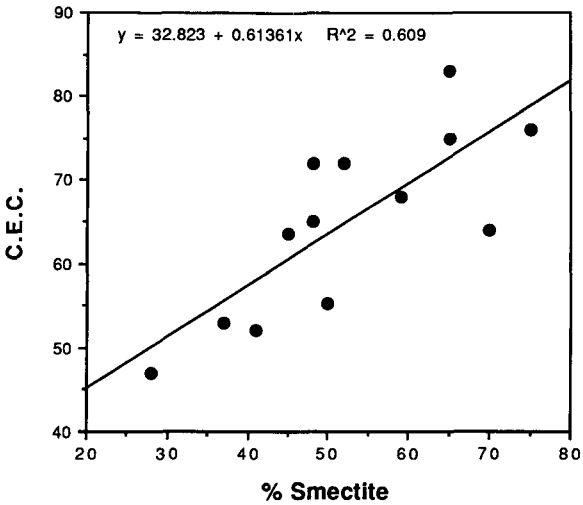

Figure 8. CEC vs. % smectite in I–S of the <0.2 μm fraction.

SiO_2 33.46%, Al_2O_3 10.96%, Fe_2O_3 2.56%, FeO 24.72%, MnO 0.4%, MgO 16.52%, CaO 0.92%, Na_2O 0.29%, H_2O 9.96%. This composition was chosen as best representing the iron-bearing chlorites so often found in sediments and sedimentary rocks. Because of the small amounts present of each of these impurities, the corrections had very little effect on the ultimate composition of the extrapolated smectite end member.

The impurity-corrected chemical data of the <0.2 μm fractions were taken to calculate the structural formulas (Marshall 1949) of the pure I–S mixed-layer minerals on the basis of 10 oxygens plus 2 hydroxyls and a total negative charge of 22. Since the samples were saturated with Na during preparation, the determined CECs of the <0.2 μm fractions were recalculated to Na_2O and included in the formula calculation. Because the primary interlayer cations are not known, the term "X^+" instead of "Na^+" is used in the formulas.

Detrital mica of an appropriate composition and present in the <0.2 μm fraction, was likewise subtracted from the composition of the structural formulas of the mixed layers. Ideal muscovite was first considered, but if indeed present would have been degraded during weathering and transport before deposition. Therefore, it seemed likely that a detrital illite was most appropriate. A composition represented by the mean of 21 sericites (Eberl et al. 1987) was chosen. Its formula is: $K_{0.76}Na_{0.02}Sr_{0.04}(Al_{1.8}Fe_{0.06}Mg_{0.13})(Si_{3.30}Al_{0.70})O_{10}OH_2$.

The estimation of small amounts of detrital mica in the presence of I–S phases with moderate to high illite content by means of XRD analyses is difficult, if not impossible. For that reason a constant value of 6% sericitic mica, which is equivalent to the uppermost sample of the drilling Puchkirchen, was removed from all samples. That is, it was assumed that detrital illite is essentially constant in these fine fractions. Further calculations showed that variations of a few percent of the sericite content are possible without greatly influencing the composition of the formulas. Similarly, assuming a muscovite composition and varying the content a few percent likewise had no significant effect on the ultimate composition of the mixed-layer phases and, more importantly, the extrapolated smectite end-member composition. The very small amounts of chlorite present precluded the possibility of observing any diagenetic changes in chlorite.

Table 2. Kaolinite and chlorite variation with depth in the <0.2 μm fraction (wt%).

Sample	Depth (m)	Kaolinite	Chlorite
2P1	801	1.5	1.5
6P1	1560	2.5	1.5
7P1	1622	3	3
8P1	1885	2.5	2.5
9P1	2065	3	3
10P1	2297	3	3
12P1	2475	2.5	2.5
27GB1	912	3	3
28GB1	1093	1	1
29GB1	1323	1.5	1.5
32GB1	1918	4.5	5.5
33GB1	2110	5.5	6.5
34GB1	2247	8.5	7.5

The resulting formulas of the I–S mixed layers of the Molasse Basin are listed in Table 3 and the distribution of the cationic charges on tetrahedral, octahedral and interlayer positions is plotted in the triangular diagram muscovite–celadonite–pyrophyllite, Figure 9 (Yoder and Eugster 1955). Figure 9 also shows the diagenetic trend from smectitic to illitic composition. The smectites do not plot in the field calculated for typical montmorillonites (Köster 1981), but show a higher interlayer charge. This is quite significant, as will be discussed later.

Gains and Losses During Burial Diagenesis

To establish the overall compositional changes of the clay minerals during diagenesis, the chemical components of the bulk chemical formulas for the mixed-layer phases were plotted as a function of smectite percent. Percent smectite was chosen, because its disappearance is an indicator of diagenesis. The results of linear regression analyses are shown in Figures 10 and 11.

Figure 10 shows a significant increase in tetrahedral charge and, therefore, tetrahedral Al^{3+} and a decrease in octahedral charge during illitization. The interlayer charge increases only slightly, indicating that the tetrahedral and octahedral substitutions essentially balance one another.

During smectite-to-illite transition, interlayer K^+ increases, whereas X^+, calculated from the CEC, de-

https://doi.org/10.1346/CCMN.1998.0460606 Published online by Cambridge University Press

Table 3. Structural formulas of the I–S mixed-layer phases (based on $O_{10}(OH)_2$). Z^+ = interlayer charge, O^- = octahedral charge, T^- = tetrahedral charge, Fe = Fe^{3+}.

Sample	Z (+)	O (−)	T (−)	Z (K)	Z (X+)	O (Al)	O (Fe)	O (Mg)	O (Ti)	T (Si)	T (Al)
2P1	0.60	0.50	0.10	0.28	0.31	1.18	0.38	0.39	0.01	3.90	0.10
6P1	0.67	0.46	0.21	0.26	0.40	1.22	0.32	0.44	0.01	3.79	0.21
7P1	0.64	0.44	0.20	0.34	0.32	1.26	0.36	0.33	0.01	3.80	0.20
8P1	0.59	0.39	0.20	0.26	0.34	1.27	0.34	0.37	0.01	3.80	0.20
9P1	0.59	0.38	0.21	0.22	0.33	1.23	0.37	0.37	0.02	3.79	0.21
10P1	0.66	0.39	0.27	0.31	0.30	1.20	0.37	0.41	0.02	3.73	0.27
12P1	0.62	0.32	0.30	0.33	0.25	1.19	0.37	0.48	0.01	3.70	0.30
27GB1	0.57	0.55	0.02	0.21	0.38	1.14	0.33	0.50	0.01	3.98	0.02
28GB1	0.61	0.61	0.00	0.22	0.35	1.02	0.41	0.53	0.01	4.00	0.00
29GB1	0.59	0.48	0.11	0.25	0.32	1.09	0.39	0.52	0.01	3.89	0.11
32GB1	0.55	0.20	0.35	0.33	0.27	1.15	0.43	0.49	0.02	3.65	0.35
33GB1	0.64	0.37	0.27	0.28	0.30	1.19	0.40	0.39	0.02	3.73	0.27
34GB1	0.67	0.48	0.19	0.37	0.27	1.17	0.33	0.49	0.01	3.81	0.19

creases (Figure 11), although the total interlayer charge barely increases (Figure 10), indicating K^+ exchange and fixation in highly charged layers. In spite of substantial replacement of octahedral Mg^{2+} by Al^{3+} (Figure 12), the coupled replacement of tetrahedral Si^{4+} by Al^{3+} (Figure 10) results in only slight change in interlayer charge.

By extrapolation of these data to 100% smectite and 100% illite, it was possible to calculate the composition of the 2 end members from the results of linear regression analyses, as shown in Figure 13. Shown here also are the gains and losses of the chemical components during diagenesis. A balanced chemical reaction, based on reaction between smectite and K-feldspar to form illite, can be written:

$$K_{0.14}X_{0.44}(Al_{1.10}Mg_{0.46}Fe_{0.36}Ti_{0.01})Si_4O_{10}(OH)_2$$
$$+ 0.64[KAlSi_3O_8] + 0.02Fe^{3+} + 4.48H_2O + 0.64H^+$$
$$\rightarrow K_{0.44}X_{0.19}(Al_{1.26}Mg_{0.42}Fe_{0.38}Ti_{0.01})Si_{3.52}Al_{0.48}O_{10}(OH)_2$$
$$+ 0.34K^+ + 0.25X^+ + 0.04Mg^{2+}$$
$$+ 2.4[H_4SiO_4]$$

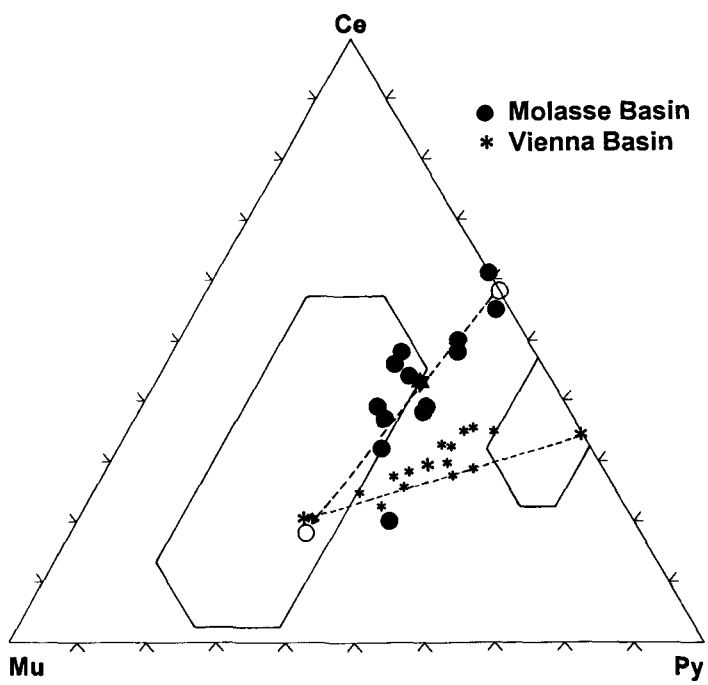

Figure 9. Comparison of the diagenetic trends of the Molasse Basin and Vienna Basin. Variation in octahedral and tetrahedral charge of the I–S plotted in the muscovite–celadonite–pyrophyllite diagram. O = end members, * = mean composition, arrow = diagenetic trend, illite (I) and smectite (S) fields (Köster 1981).

https://doi.org/10.1346/CCMN.1998.0460606 Published online by Cambridge University Press

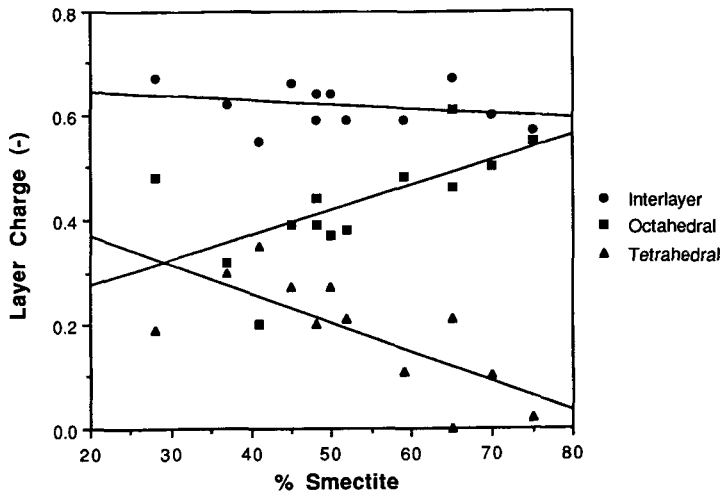

Figure 10. Tetrahedral, octahedral, interlayer charge vs. % smectite in I–S.

DISCUSSION

Detailed studies of these Molasse Basin clay-silt sediments have revealed a diagenetic overprint, involving gradual transformation of smectite to illite through mixed-layer I–S intermediates within the fine clay mineral matrix. This is in agreement with the shallowest zone 1 (1.85 to 3 km) described by Eberl 1993, where the gradual decrease in expandability is thought to result from K^+ ion exchange transformation mechanism for illite layer formation, in which high-charged smectite layers coalesced around interlayer K^+. The increase in layer charge is due to substitution of Al^{3+} for Si^{4+} in the smectite tetrahedral sheet.

The illitization of the investigated I–S clay minerals of the Molasse Zone of Upper Austria has produced up to 70% illitic layers in the mixed-layer I–S. The I–S phases are randomly interlayered to a depth of 1600 m; below that, to a depth of 2500 m, there is evidence of ordered I–S coexisting with randomly ordered I–S. These results are slightly different from other investigations of I–S mixed-layer minerals of Tertiary basins of the world (Hower et al. 1976; Johns and Kurzweil 1979; Awwiller 1993; Sucha et al. 1993; Lynch 1997), because of the continuing existence of randomly interlayered I–S to a depth of 2500 m.

The main factor controlling the extent of conversion of smectite to illite is the temperature and also the length of time the shale has been buried (Hower et al. 1976). The calculated geothermal gradient for the wells Puchkirchen 1 and Geretsberg 1 is 2.9 °C/100 m. This is in accordance with the general gradient of 3 °C/100 m for the Molasse Basin (Kunz 1978). In the East-Slovak Basin, the transition from random to ordered I–S interstratification takes place at a depth of

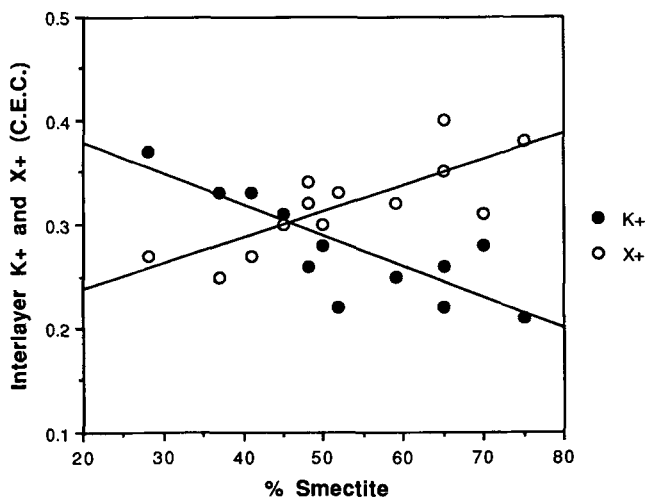

Figure 11. Interlayer K^+, X^+ vs. % smectite in I–S.

https://doi.org/10.1346/CCMN.1998.0460606 Published online by Cambridge University Press

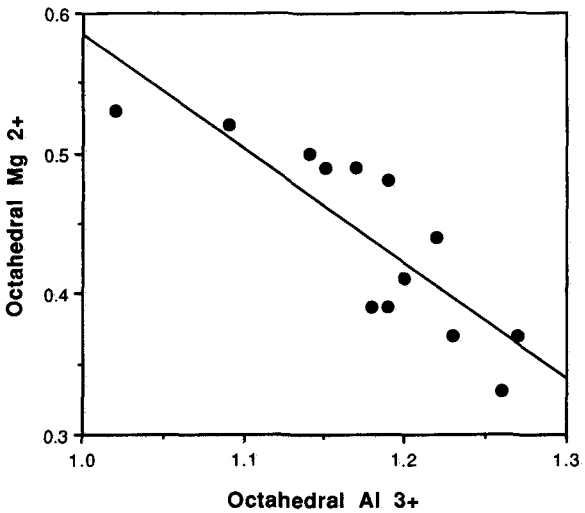

Figure 12. Octahedral Al^{3+} vs. octahedral Mg^{2+} in I–S.

1800 m at an expandable layer content of 35–40%. The geothermal gradient there is about 5 °C/100 m (Sucha et al. 1993). By comparison, the geothermal gradient of the Molasse Basin is low and this is probably the reason why there are still randomly interlayered I–S mixed-layer minerals at depths of 2500 m.

In another respect, the I–S transformation here is quite different from that observed previously elsewhere. In particular, the detailed chemical studies of the I–S phases indicate that the initial smectite component exhibits a high interlayer charge (+0.58), approaching that of a vermiculite (dioctahedral) with more celadonitic composition and higher Fe^{3+} content than conventional low-charged smectites.

Also as emphasized in Figure 9, where the diagenetic trend is indicated, there is only a very slight increase in interlayer charge, indicating that the coupled substitution of Al^{3+} for tetrahedral Si^{4+} and octahedral Mg^{2+} results in interlayer charge maintenance, accompanying K^+-fixation.

This is in marked contrast to the Vienna Basin of Austria (Horton et al. 1985), Figure 9, where the illitization trend involves increasing interlayer charge, resulting from substitution of Al^{3+} for Si^{4+} and to a much lesser extent for Mg^{2+}, thus resulting in progressive increase in interlayer charge, starting with a low-charge smectite (+0.38) precursor.

Earlier studies of K-fixation (Eberl et al. 1986) and NH_4-fixation (Sucha and Siranova 1991) in smectites after saturation and repeated wetting and drying cycles, had indicated that, in the case of pure smectites, high-charged varieties (>0.40 per $O_{10}(OH)_2$) are usually a mixture of a high- and low-charged component. Also, alkylammonium ion orientation studies in smectites revealed a mixed-layer type structure of higher and lower charged smectite layers (Lagaly and Weiss 1976; Stul and Mortier 1974).

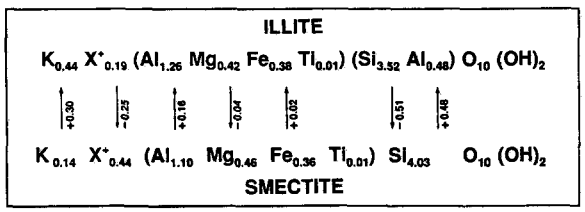

Figure 13. End members smectite and illite, gains and losses of the chemical components during diagenesis.

This supports the growing realization that many I–S phases involved in burial diagenesis contain a smectite component with high interlayer charge and that these I–S phases are indeed intergrowths of 3 layer-silicate members: illite, low-charged smectite and high-charged smectite. It appears likely that the high-charged end-member smectite from the Puchkirchen and Geretsberg series is also a mixture of 2 smectite components of widely different layer charge. The high-charged component, vermiculite-like in terms of charge, would presumably have readily transformed to illite during diagenesis, except for a lack of sufficient K^+. The low-charged, normal smectite component would require more extensive transformation, additional K^+-fixation and Al^{3+} for Si^{4+} substitution to change to illite. Two mechanisms for illitization would be required.

It is likely that future studies will show similar variations, which undoubtedly reflect differences in source material leading to the formation of different early, highly smectitic I–S phases in sedimentary basins.

To confirm these presumptions, further detailed investigations of K-fixation and alkylammonium ion orientation in this I–S series are in progress by the author.

ACKNOWLEDGMENTS

The author thanks the RAG AG for providing the drill core samples. I wish to thank W. D. Johns for the valuable discussions and the critical reading of the manuscript. I am grateful to H. Kurzweil for initiating this work and for his very helpful suggestions. I also want to acknowledge P. Dolezel (BFPZ Arsenal) for carrying out the ICP-analysis.

REFERENCES

APD 3.5B. 1992. PC-APD 3.5B, Philips PW 1877 Automated powder diffraction. Holland.

Association Nationale de la Recherche Technique. 1989. Geostandards newsletter 13 (Special Issue):23.

Awwiller DN. 1993. Illite smectite formation and potassium mass transfer during burial diagenesis of mudrocks: A study from the Texas Gulf Coast Paleocene-Eocene. J Sed Pet 63:501–512.

Bruce CH. 1984. Smectite dehydration—Its relation to structural development and hydrocarbon accumulation in northern Gulf of Mexico Basin. AAPG Bull 68:673–683.

Burst JF. 1969. Diagenesis of Gulf Coast clayey sediments and its possible relation to petroleum migration. AAPG Bull 53:73–93.

Busenberg E, Clemency CV. 1973. Determination of the cation exchange capacity of clays and soils using an ammonia electrode. Clays Clay Miner 21:213–217.

Deer WA, Howie RA, Zussman J. 1962. Rock-forming minerals—Sheet silicates, vol. 3. Longmans.

Eberl DD. 1993. Three zones for illite formation during burial diagenesis and metamorphism. Clays Clay Miner 41:26–37.

Eberl DD, Środoń J, Mingchou L, Nadeau PH, Northrop HR. 1987. Sericite from the Silverton caldera, Colorado: Correlation among structure, composition, origin and particle thickness. Am Mineral 72:914–934.

Eberl DD, Środoń J, Northrup HR. 1986. Potassium fixation in smectite by wetting and drying. In: Davis JA, Hayes KF, editors. Geochemical processes at mineral surfaces. Am Chem Soc Symposium Series 323:296–326.

Glover ED. 1961. Method of solution of calcareous materials using the complexing agent, EDTA. J Sed Pet 31:622–626.

Horton RB, Johns WD, Kurzweil H. 1985. Illite diagenesis in the Vienna Basin, Austria. TMPM 34:239–260.

Hower J, Eslinger EV, Hower ME, Perry EA. 1976. Mechanism of burial metamorphism of argillaceous sediment: 1. Mineralogical and chemical evidence. Geol Soc Am Bull 87:725–737.

Jasmund K, Lagaly G. 1993. Tonminerale und Tone. Darmstadt: Steinkopff. 490 p.

Johns WD, Kurzweil H. 1979. Quantitative estimation of illite–smectite mixed-phases formed during burial diagenesis. TMPM 26:203–215.

Kohler E, Wewer R. 1980. Gewinnung reiner Tonmineralkonzentrate für die mineralogische Analyse. Keramische Zeitschrift 32 Nr. 5:250–252.

Köster HM. 1979. Die chemische Silikatanalyse. Berlin: Springer-Verlag. 196 p.

Köster HM. 1981. The crystal structure of 2:1 layer silicates. In: Van Olphen H, Veniale F, editors. Developments in sedimentology. Proc Int Clay Conf; 1981. Amsterdam: Elsevier. p 41–71.

Kunz B. 1978. Temperaturmessungen in Erdölbohrungen der Molassezone Oberösterreichs. Mitt Österr Geol Ges 68:51–58.

Kurzweil H. 1973. Sedimentpetrologische Untersuchungen an den jungtertiären Tonmergelserien der Molassezone Oberösterreichs. TMPM 20:169–215.

Kurzweil H, Johns WD. 1981. Diagenesis of tertiary marlstones in the Vienna Basin. TMPM 29:103–125.

Lagaly G, Weiss A. 1976. The layer charge of smectitic layer silicates. Proc Int Clay Conf; Mexico City; 1975. p 157–172.

Lynch, FL. 1997. Frio shale mineralogy and the stoichiometry of the smectite to illite reaction: The most important reaction in clastic sedimentary diagenesis. Clays Clay Miner 45:618–631.

Malzer O, Rögl F, Seifert P, Wagner L, Wessely G, Brix F. 1993. Die Molassezone und deren Untergrund. In: Brix F, Schultz O, editors. Erdöl und Erdgas in Österreich. Wien: NHM Wien. p 281–323.

Marshall CE. 1949. The structural interpretation of chemical analyses of the clay minerals. In: The colloid chemistry of the silicate minerals. New York: Academic Pr. 159 p.

Moore DM, Reynolds RC Jr. 1989. X-ray diffraction and the identification and analysis of clay minerals. New York: Oxford Univ Press. 332 p.

Perry EA, Hower J. 1972. Late-stage dehydration in deeply buried pelitic sediments. AAPG Bull 56:2013–2021.

Powers MC. 1967. Fluid-release mechanisms in compacting marine mudrocks and their importance in oil exploration. AAPG Bull 51:1240–1254.

Reynolds RC Jr. 1985. NEWMOD©, a computer program for the calculation of one-dimensional diffraction patterns of mixed-layered clays. R. C. Reynolds, Jr.: 8 Brook Drive, Hanover, NH.

Reynolds RC Jr. 1989. Principles and techniques of quantitative analysis of clay minerals by X-ray powder diffraction. In: Pevear DR, Mumpton FA, editors. Quantitative mineral analysis of clays, CMS Workshop Lectures, vol. 1. Boulder, CO: Clay Miner Soc. p 4–36.

Schultz LG. 1964. Quantitative interpretation of mineralogical composition from X-ray and chemical data for Pierre shale. Washington. US Geol Survey. Prof Paper 391-C.

Stul MS, Mortier WJ. 1974. The heterogeneity of the charge density in montmorillonites. Clays Clay Miner 22:391–396.

Sucha V, Kraus I, Gerthofferova H, Petes J, Serekova M. 1993. Smectite to illite conversion in bentonites and shales of the East Slovak Basin. Clay Miner 28:243–253.

Sucha V, Siranova V. 1991. Ammonium and potassium fixation in smectite by wetting and drying. Clays Clay Miner 39:556–559.

Tollmann A. 1985. Die Molassezone. Geologie von Österreich. Band 2. Wien: Verlag Franz Deuticke. 710 p.

Yoder HS, Eugster HP. 1955. Synthetic and natural muscovites. Geochim Cosmochim Acta 8:225–280.

(Received 30 August 1996; accepted 1 April 1998; Ms. 2807)